

## Simulation of Space Experiments for Nuclear Planetology

### Measurement of Relative Intensities of Lines of Gamma Ray Emitted upon Thermal-Neutron Capture by Nuclei

Kozyrev, A. S.; Anikin, A. A.; Vostrukhin, A. A.; Golovin, D. V.; Granja, C.; Dubasov, P. A.; Zontikov, A. O.; Quarati, F.; Lisov, D. I.; Owens, A.

**DOI**

[10.1134/S1063778818040099](https://doi.org/10.1134/S1063778818040099)

**Publication date**

2018

**Document Version**

Final published version

**Published in**

Physics of Atomic Nuclei

**Citation (APA)**

Kozyrev, A. S., Anikin, A. A., Vostrukhin, A. A., Golovin, D. V., Granja, C., Dubasov, P. A., Zontikov, A. O., Quarati, F., Lisov, D. I., Owens, A., & More Authors (2018). Simulation of Space Experiments for Nuclear Planetology: Measurement of Relative Intensities of Lines of Gamma Ray Emitted upon Thermal-Neutron Capture by Nuclei. *Physics of Atomic Nuclei*, 81(5), 527-539. <https://doi.org/10.1134/S1063778818040099>

**Important note**

To cite this publication, please use the final published version (if applicable).  
Please check the document version above.

**Copyright**

Other than for strictly personal use, it is not permitted to download, forward or distribute the text or part of it, without the consent of the author(s) and/or copyright holder(s), unless the work is under an open content license such as Creative Commons.

**Takedown policy**

Please contact us and provide details if you believe this document breaches copyrights.  
We will remove access to the work immediately and investigate your claim.

---

---

NUCLEI  
Experiment

---

---

## Simulation of Space Experiments for Nuclear Planetology: Measurement of Relative Intensities of Lines of Gamma Ray Emitted upon Thermal-Neutron Capture by Nuclei

A. S. Kozyrev<sup>1)\*</sup>, A. A. Anikin<sup>1)</sup>, A. A. Vostrukhin<sup>1)</sup>, D. V. Golovin<sup>1)</sup>,  
C. Granja<sup>2)</sup>, P. A. Dubasov<sup>3)</sup>, A. O. Zontikov<sup>3)</sup>, F. Quarati<sup>4)</sup>, D. I. Lisov<sup>1)</sup>,  
M. L. Litvak<sup>1)</sup>, I. G. Mitrofanov<sup>1)</sup>, A. Owens<sup>5)</sup>, S. Pospisil<sup>6)</sup>,  
A. B. Sanin<sup>1)</sup>, T. Slavicek<sup>2)</sup>, G. N. Timoshenko<sup>3),6)</sup>, and V. N. Shvetsov<sup>3)</sup>

Received January 30, 2018

**Abstract**—The results obtained by experimentally studying gamma rays emitted by samples prepared as analogs of planetary matter and irradiated with thermal neutrons are presented. The intensities of spectral lines of gamma rays emitted by such samples differing in chemical composition are compared. These results will be used in processing data on gamma-ray spectra of the Moon and Mercury from measurements performed onboard spacecrafts with the aim of studying the composition of the surface of these celestial bodies.

**DOI:** 10.1134/S1063778818040099

### 1. INTRODUCTION

Investigations on board spacecrafts into the composition of planet surfaces by means of the remote spectroscopy of neutron and gamma-ray fluxes have been performed for more than 50 years (see, for example, [1, 2]). This method is based on measuring the energy spectrum of neutron fluxes over a wide energy range from thermal energies (below an electronvolt) to fast-neutron energies of 5 to 10 MeV and the spectrum of gamma-ray fluxes in the energy range from 100 keV to 10 MeV. Neutrons and gamma rays are produced in the celestial-body surface layer about one to two meters in thickness under the effect of galactic cosmic rays (GCR) [3]. Product neutrons undergo moderation because of collisions with matter nuclei and acquire energies within a wide range extending from thermal energies to a few tens of MeV

units. A significant portion of neutrons escape from the surface and, in the absence of an atmosphere (as in the case of the Moon and Mercury) or under conditions of a thin atmosphere (as in the case of Mars), may reach altitudes of spacecraft orbits. Gamma rays originate from inelastic-scattering reactions or from neutron capture by nuclei of main rock-forming elements; also, radioactive potassium, thorium, and uranium isotopes contribute to gamma-ray emission from celestial-body matter. The spectral content of gamma rays emitted from the planet surface is determined primarily by main rock-forming elements of the surface layer. For example, the presence of iron in the surface layer leads to the emission of the 5920-, 7631-, and 7645-keV gamma lines of this element. The presence of hydrogen nuclei in the surface layer causes an effective thermalization of emitted neutrons and the emission of 2223-keV photons originating from neutron capture by hydrogen nuclei [4].

Analyzing data from measurements of neutron and gamma-ray fluxes from planet surfaces, one can determine the presence of one element or another in the surface layer on the basis of identified gamma lines and evaluate the mass fraction of these elements in soil on the basis of the radiation intensity of these lines. The detection of gamma lines associated with radioactive potassium (<sup>40</sup>K) and products of <sup>232</sup>Th and <sup>238</sup>U decay permits estimating their concentrations in the celestial body under study and clarifying thereby conditions of its origin and evolution [5].

---

<sup>1)</sup>Space Research Institute, Russian Academy of Sciences, Profsoyuznaya ul. 84/32, Moscow, 117997 Russia.

<sup>2)</sup>Institute of Experimental and Applied Physics, Czech Technical University in Prague, Horska 3a/22, 12800 Prague 2, Czech Republic.

<sup>3)</sup>Joint Institute for Nuclear Research, ul. Joliot-Curie 6, Dubna, Moscow oblast, 141980 Russia.

<sup>4)</sup>AP, RST, FAME, Delft University of Technology, Mekelweg 15, 2629 JB Delft, The Netherlands.

<sup>5)</sup>European Space Agency, ESTEC, Keplerlaan, 2200 AG Noordwijk, The Netherlands.

<sup>6)</sup>Dubna State University, Universitetskaya ul. 19, Dubna, Moscow oblast, 141982 Russia.

\*E-mail:kozyrev@cosmos.ru

Thus, the application of the nuclear-planetology method to studying the elemental composition of the celestial-body surface requires the detection of gamma rays with a rather high energy resolution that enables searches for and an identification of gamma lines that characterize the elemental composition of surface-layer matter. By means of this method, measurements of gamma-ray fluxes on board the Mars Odyssey, Lunar Prospector, and MESSENGER spacecrafts were performed in orbits of Mars, the Moon, and Mercury. This made it possible to identify the main rock-forming elements (such as Si, Mg, Al, Fe, Ca, Cr, and Ti) of the surfaces of these celestial bodies [6–8].

From the energy-resolution point of view, a gamma-ray spectrometer on the basis of a High-Purity Germanium (HPGe) detector is optimal. Its energy resolution is about 1.8 keV for the 662-keV line of  $^{137}\text{Cs}$ . This energy resolution is 15 to 20 times higher than that of gamma-ray spectrometers based on traditional NaI and CsI scintillation crystals. Space-science experiments within the Mars Odyssey, MESSENGER, and Japanese lunar orbiter SELENE (Kaguya) projects aimed at studying the elemental composition of the surface layer of Mars, Mercury and the Moon [3, 9, 10] were based on the use of HPGe spectrometers. However, HPGe spectrometers have two serious drawbacks that complicate their application in experiments on board spacecrafts for nuclear-planetology studies. First, the energy resolution of germanium crystals becomes lower under the effect of charged cosmic-ray particles. Solar proton events exert the strongest influence of this kind. In order to restore the energy resolution of HPGe-based detectors, it is necessary to implement a hazardous annealing procedure that involves heating the germanium crystal used to temperatures of about  $100^\circ\text{C}$ . Second, physics measurements with HPGe-based detectors are performed only at crystal temperatures below  $-180^\circ\text{C}$ . In order to ensure this thermal regime, it is necessary to have a passive or an active system of cryogenic cooling, but this requires additional masses and entails an additional energy consumption.

In view of the above special features of HPGe-based detectors, detectors on the basis of scintillation crystals, such as NaI, CsI, and BGO whose energy resolution for the 662-keV line of the isotope  $^{137}\text{Cs}$  are, respectively, about 6% to 8%, 7.0% to 8.5%, and 10% to 13% [11], were mostly used in space-science experiments devoted to gamma-ray spectroscopy. At the present time, researchers have at their disposal better detectors on the basis of  $\text{LaBr}_3$ ,  $\text{LaCl}_3$ , or  $\text{CeBr}_3$  crystals whose energy resolution for the above line is 3% to 4%. Such gamma-ray spectrometers are

still inferior in energy resolution to HPGe-based detectors, but the former are preferable in space-science applications, where reliability, mass-minimization, and energy-consumption requirements come to the fore. For example, the HPGe-based gamma-ray spectrometer for the MESSENGER spacecraft had a weight of about 9.2 kg and consumed about 16.5 W (about 23.0 W in the annealing regime). A scintillation gamma-ray spectrometer based on a  $\text{CeBr}_3$  (or  $\text{LaBr}_3$ ) crystal and characterized by a commensurate efficiency may have a mass not higher than 4 kg and consume not more than 3.5 W. Such an instrument would permit reducing the expenditure of the onboard resources by a factor of 2.3 in mass and by a factor of 6.5 in energy consumption. Frequently, this circumstance is of importance in designing automated interplanetary spacecrafts.

In view of the aforementioned circumstances, the Russian MGNS (Mercury Gamma-ray and Neutron Spectrometer) instrument based on a  $\text{CeBr}_3$  innovative crystal [12, 13] was incorporated in the Bepi-Colombo satellite of the European Space Agency (ESA) project devoted to studying Mercury. The scientific objectives of this experiment include a global mapping of the elemental composition of the Mercury surface layer. In order to fulfil this task, the spectra of gamma rays emitted from various surface regions of this celestial body will be measured from an orbit. The processing of these spectra will be aimed at identifying spectral lines characteristic of nuclei of main rock-forming elements and at determining their mass fraction in celestial-body matter.

A relatively small signal-to-background ratio for many gamma-ray lines and the superimposition of the profiles of lines close in energy because of an insufficiently high energy resolution of the instrument used are the main problems encountered in processing the measured spectra of gamma rays emitted from celestial-body surfaces.

The present article reports on a laboratory experiment performed at an Experimental Facility for Nuclear Planetology (EF-NP-03) and aimed at measuring reference gamma-ray lines arising in nuclear reactions of thermal-neutron capture in samples prepared as analogs of celestial-body matter. These measurements were performed by means of a scintillation gamma-ray spectrometer equipped with a detector on the basis of  $\text{CeBr}_3$ . The experimental program is restricted to studying lines associated with neutron-capture reactions since fluxes of thermal neutrons from celestial-body surfaces are measured quite reliably in space-science experiments devoted to the gamma-ray spectroscopy of planets. Via a comparison of data on the intensities of lines from specific nuclei with data on thermal-neutron fluxes, one will be able to estimate the concentration of these

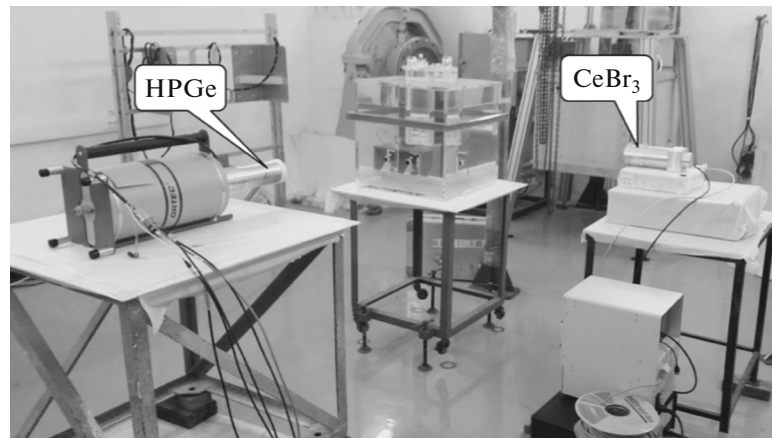


Fig. 1. EF-NP-03 laboratory setup.

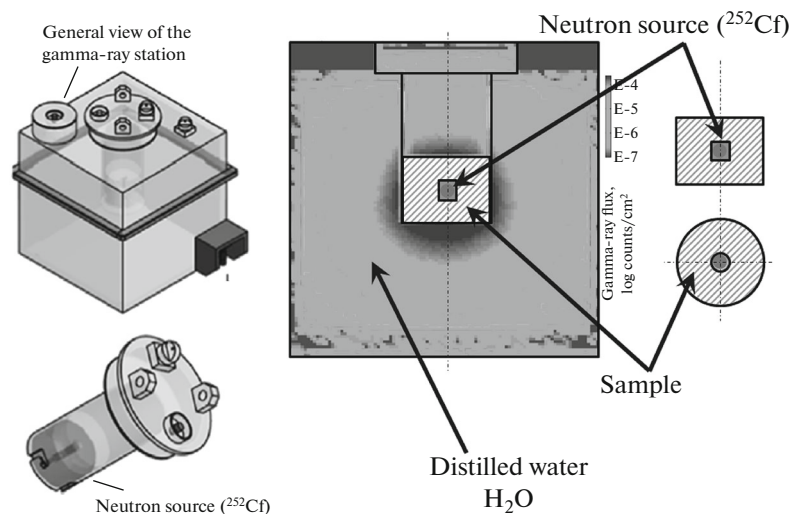


Fig. 2. Layout of the gamma-ray station as a source of secondary gamma rays.

nuclei in matter. In the future, data obtained in the EF-NP-03 experiment will make it possible to identify basic neutron-capture gamma-ray lines from the Mercury surface that are measured by the MGNS instrument, to measure their intensities, and to determine the concentration of rock-forming elements in Mercurian soil that correspond to these lines.

The EF-NP-03 laboratory setup includes gamma-ray spectrometers on basis of a  $\text{CeBr}_3$  scintillation crystal and on the basis of HPGe and a dedicated gamma-ray station, which, in turn, serves as a source of epithermal and thermal neutrons whose spectrum is analogous to the spectrum of secondary neutrons arising in the upper layer of the surface of atmosphere-free celestial bodies under the effect of galactic cosmic rays [14]. Thermal-neutron density reaches a maximum value in the central region of the gamma-ray station. Samples of various chemical composition simulating celestial-body matter were

placed in this region. The inclusion of an HPGe-based spectrometer in EF-NP-03 makes it possible to reveal a nearly whole set of spectral gamma-ray lines for each sample mimicking celestial-body matter and to perform a comparison with spectral

Table 1. Composition of the Soil 1 (1605 g) and Soil 2 (1585 g) samples

| Oxide  | Soil 1  |         | Soil 2  |         |
|--|---------|---------|---------|---------|
|  | mass, % | mass, g | mass, % | mass, g |
| $\text{SiO}_2$   | 64.4    | 1033.6  | 82.9    | 1314.0  |
| $\text{Al}_2\text{O}_3$  | 13.0    | 208.7   | 10.6    | 168.0   |
| $\text{Na}_2\text{O}, \text{MgO}, \text{P}_2\text{O}_5,$<br>$\text{K}_2\text{O}, \text{TiO}_2, \text{MnO},$<br>$\text{Fe}_2\text{O}_3, \text{CaO}$ | 22.6    | 362.7   | 6.5     | 103.0   |

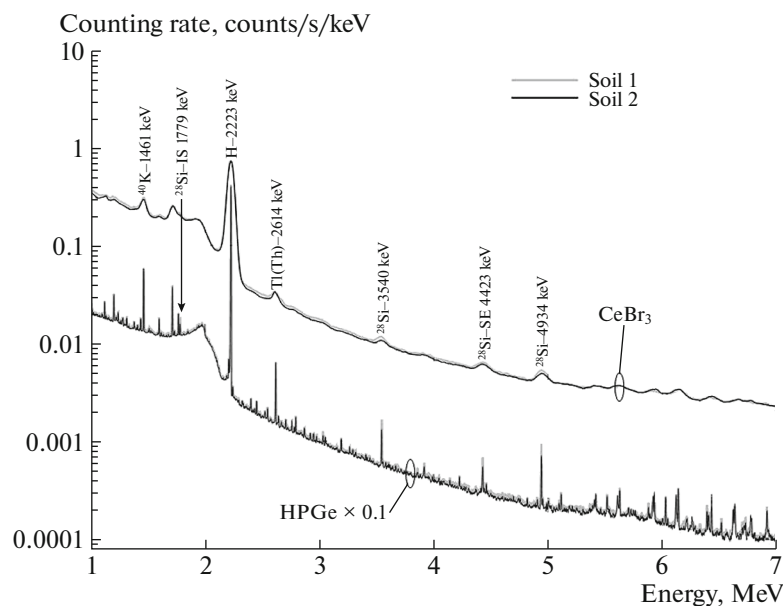


**Fig. 3.** Spectra of gamma rays from the Soil 1 and Soil 2 samples according to measurements by means of the gamma-ray spectrometers based on HPGe and on a  $\text{CeBr}_3$  crystal.

details measured by the detector on the basis of cerium bromide. Samples that are analogous to celestial-body matter and which contain oxides of various rock-forming elements were manufactured for measurements.

## 2. DESCRIPTION OF THE LABORATORY SETUP

The EF-NP-03 laboratory setup was created at the Laboratory of Neutron Physics at the Joint Institute for Nuclear Research (JINR, Dubna) by a collaboration including physicists from Space Research Institute (IKI, Moscow, Russian Academy of Sciences) and Institute for Experimental and Applied Physics (Czech Technical University, Prague) as part of a research project supported by Russian Science Foundation (RSF grant no. 14-22-00249). The EF-NP-03 setup includes a gamma-ray source based on a portable gamma-ray station [14], where primary neutrons from a  $^{252}\text{Cf}$  radioactive source undergo moderation in a water-filled tank to epithermal and thermal energies. The gamma-ray station generates its own gamma radiation from a radioactive source and from neutron-capture reactions occurring in water and in structural elements. A holder for samples playing the role of analogs of celestial-body matter is positioned in the central region of the gamma-ray station. The detecting block of the setup comprises gamma-ray spectrometers based on a  $\text{CeBr}_3$  scintillation detector and a HPGe semiconductor detector (Fig. 1).

The gamma-ray station has the form of a parallelepiped whose outer dimensions are  $50 \times 56 \times 56$  cm. It is filled with distilled water 110 l in volume. The parallelepiped walls were fabricated from poly(methyl methacrylate) (plexiglass). The holder containing the sample under study and a  $^{252}\text{Cf}$  neutron source is arranged at the geometric center of the parallelepiped (Fig. 2). The activity of this neutron source in the course of the measurements was  $1.95 \times 10^6$  neutron/s. The spectrum of neutrons emitted in the spontaneous fission of  $^{252}\text{Cf}$  is well described by a Maxwellian distribution characterized by a mean energy of  $2.13 \pm 0.01$  MeV [15].

The gamma-ray spectrometers are installed on mutually orthogonal directions with respect to the gamma-ray station at identical distances of about 1 m from its center. This symmetric geometry permits simultaneously measuring gamma rays from one sample with two gamma-ray spectrometers under conditions of identical radiation fluxes incident to detectors (see Fig. 1).

The scintillation gamma-ray spectrometer for EF-NP-03 includes a detector  $\varnothing 3 \times 3$  in size based on a  $\text{CeBr}_3$  crystal and specially manufactured for the experiment in question, as well as an R1307-13 photomultiplier tube (PMT). The scintillation-crystal dimensions, electrical circuits of a high-voltage divider, and the inner structure of the scintillation block faithfully reproduce the structure of the gamma-ray detector in the MGNS instrument. The electronics equipment of the gamma-ray spectrometer was implemented on the basis of prefabricated industrial units of the ORTEC company. The logical scheme of

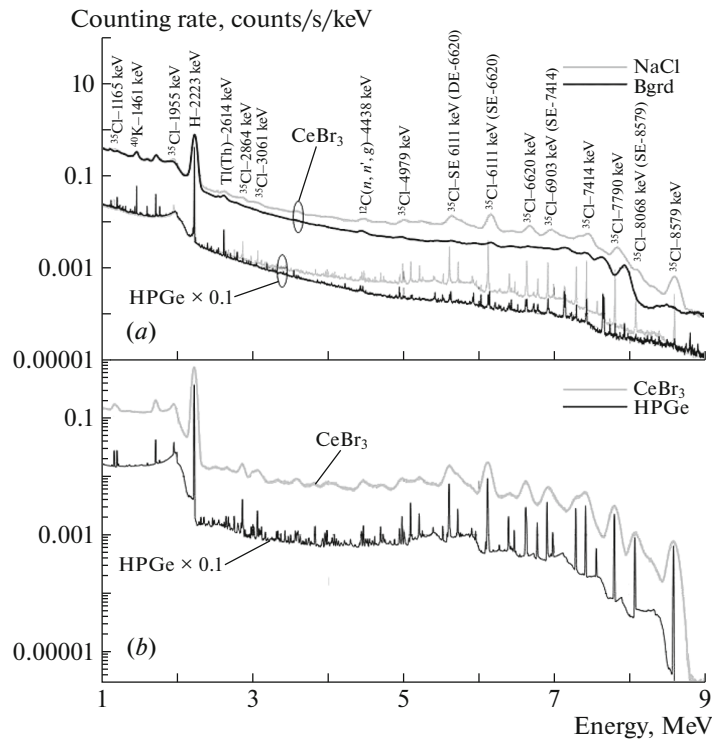


**Fig. 4.** Spectra of gamma rays from a NaCl sample (*a*) according to measurements with the gamma-ray spectrometers based on HPGe and on a CeBr<sub>3</sub> crystal and (*b*) according to a simulation for the gamma-ray spectrometers based on HPGe and on a CeBr<sub>3</sub> crystal.

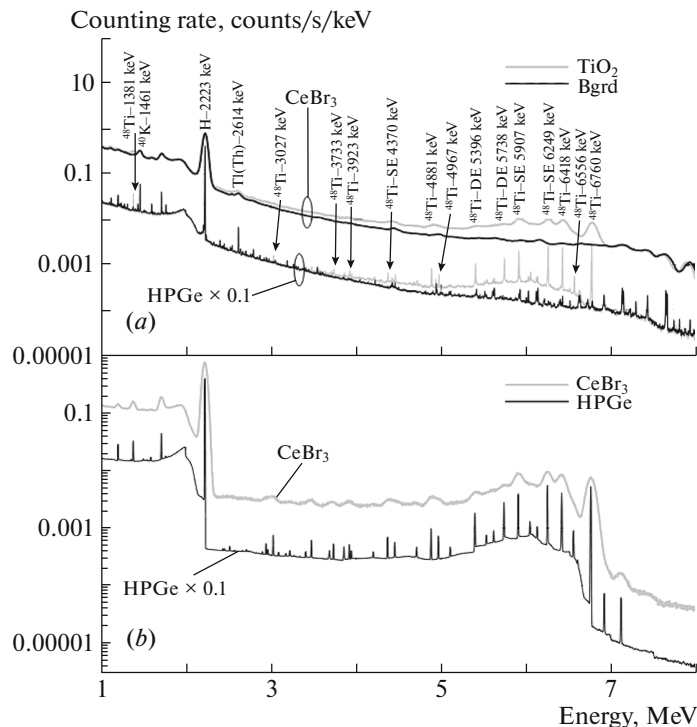


**Fig. 5.** As in Fig. 4, but for a TiO<sub>2</sub> sample.

the gamma-ray spectrometer makes it possible to accumulate instrumental spectra in 4096 channels. The energy resolution of the gamma-ray spectrometer is about 29 keV (4.4%) for the 662-keV line of <sup>137</sup>Cs.

In order to measure gamma rays with a high energy resolution, an industrial gamma-ray spectrometer on the basis of an HPGe crystal  $\varnothing 66 \times 89$  mm in size manufactured by the ORTEC company was

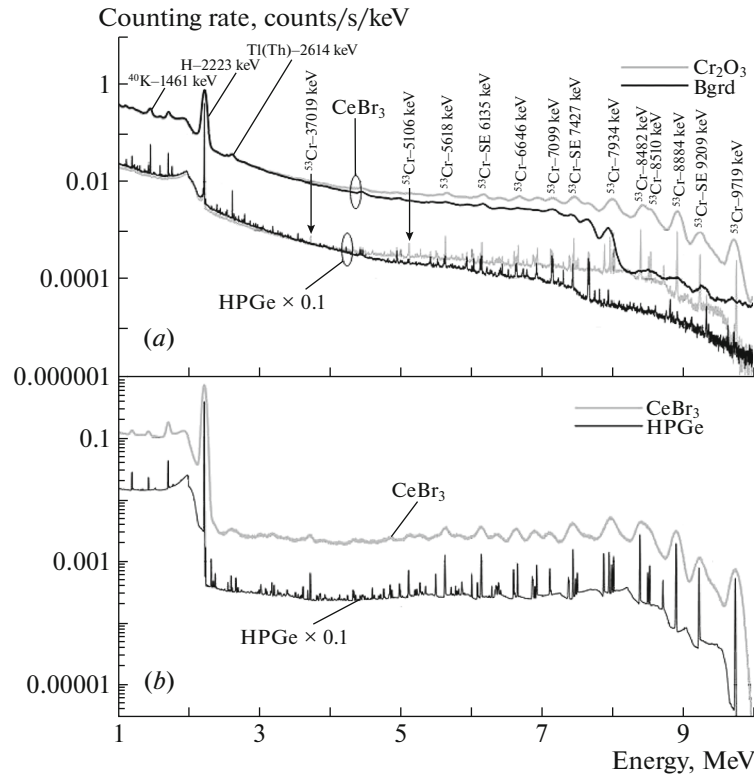


Fig. 6. As in Fig. 4, but for a  $\text{Cr}_2\text{O}_3$  sample.

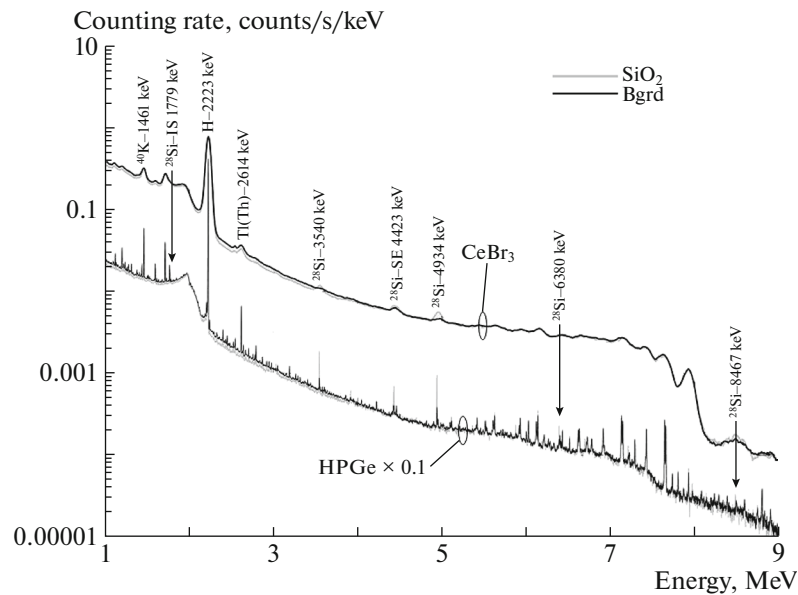


Fig. 7. Spectra of gamma rays from a  $\text{SiO}_2$  sample according to measurements by means of the gamma-ray spectrometers based on HPGe and on a  $\text{CeBr}_3$  crystal. The gamma-ray spectra measured for the gamma-ray source without a sample are shown in black.

used in the EF-NP-03 setup. The energy resolution of this spectrometer is 1.8 keV (about 0.27%) for the 662-keV gamma line of  $^{137}\text{Cs}$  and 2.2 keV (about 0.17%) for the 1332-keV gamma line of  $^{60}\text{Co}$ . The

laboratory gamma-ray spectrometer also includes a 16 384-channel amplitude analyzer.

Fast neutrons from the  $^{252}\text{Cf}$  source undergo multiple elastic scattering off hydrogen nuclei contained in water molecules. These collisions lead to quite an

efficient moderation of emitted neutrons and to the formation of a high density of epithermal and thermal neutrons at the source center. Thermal neutrons are readily captured by nuclei of the sample material, which, in the capture process, emit gamma rays of fixed energy (gamma-ray lines). After going out of the gamma-ray station, gamma rays are detected by the spectrometers. Thus, a set of gamma-ray lines is associated with each sample simulating celestial-body matter.

A simultaneous application of scintillation and semiconductor detectors makes it possible to identify all distinct features of the spectra measured with the aid of a scintillator and to obtain a list of basic detected gamma-ray lines for each sample used as an analog of celestial-body substances. Moreover, a comparison of data from measurements with detectors of these two types enables one to confirm that the scintillation detector based on a  $\text{CeBr}_3$  crystal has a sensitivity and a spectral resolution that are sufficient for studying the composition of celestial bodies.

It is noteworthy that, in addition to gamma-ray lines characteristic of the sample under study, the measured spectra contain gamma-ray lines from neutron-irradiated elements of the gamma-ray station itself, the whole experimental setup, and the hall in which the measurements were performed. In order to take into account the contribution of these gamma-ray lines, background measurements without any sample in the holder of the gamma-ray station were performed in the course of the experiment. The 2223-keV line emitted upon neutron capture by a hydrogen nucleus (proton) transforming as a result into a deuteron is the brightest background gamma-ray line (see Fig. 3–8). A high intensity of this gamma-ray line is due to a large amount of water surrounding the neutron source.

Purified- and analytical-grade (mass fraction of the main substance not lower than 96%) oxides of various chemical elements were used as analogs of celestial-body matter. Characteristic sample masses ranged between 850 and 1600 g.

### 3. IMPLEMENTATION OF MEASUREMENTS AND ANALYSIS OF RESULTS

At the first stage of the experiment, we performed measurements for two natural-soil samples (see Fig. 3) of permafrost test sites provided by the Melnikov Permafrost Institute (MPI, Siberian Branch, Russian Academy of Sciences) [16]. The composition of these samples was studied at Institute of Microelectronics Technology and High-Purity Materials (Russian Academy of Sciences) by means of mass spectrometry and by the atomic-emission method. The composition of these samples is given

in Table 1. For either natural-soil sample under study, the spectra of gamma rays were measured by both gamma-ray spectrometers. The results of those measurements are presented in Table 2.

The main oxide in the samples is  $\text{SiO}_2$ , whose mass fraction is 64% and 83% for, respectively, the Soil 1 and Soil 2 samples (see Table 1). The masses of these samples are 1605 and 1585 g; therefore, the partial mass fraction of the silicon oxide in the Soil 1 and Soil 2 samples is 1034 and 1314 g, respectively. Thus, the Soil 2 sample is 1.3 times richer in silicon oxide than the Soil 1 sample. The most intense gamma-ray lines of  $^{28}\text{Si}$  at the energies of 3540, 4423 (SE), and 4934 keV were detected in both gamma-ray spectrometers (HPGe and  $\text{CeBr}_3$ ). Their intensities were higher for the Soil 2 sample (see Fig. 3). In addition to silicon lines, the spectrometers recorded a gamma line associated with aluminum oxide, which is the second oxide in mass in soil (see Table 1). Its partial mass in the samples is 209 and 168 g for Soil 1 and Soil 2, respectively. Because of a small number of aluminum nuclei in the samples, the 7724-keV gamma-ray line of  $^{27}\text{Al}$  from the radiative-capture reaction was detected only by the HPGe semiconductor gamma-ray spectrometer. Gamma lines from the other oxides entering into the composition of the Soil 1 and Soil 2 samples (see Table 1) were not detected, since their intensities proved to be overly low for detection in the setup used because of an insufficient oxide mass in the samples being studied. In view of this, subsequent measurements were performed for samples consisting of monoxides.

For the second stage of the experiment, we selected oxides of seven elements entering into the composition of Martian [17] and Mercurian [18] regolith:  $\text{SiO}_2$ ,  $\text{CaO}_2$ ,  $\text{Cr}_2\text{O}_3$ ,  $\text{MnO}_2$ ,  $\text{TiO}_2$ ,  $\text{P}_2\text{O}_5$ , and  $\text{Al}_3\text{O}_3$ . In addition to these oxides, chlorine is of particular interest, since it is known to be contained in Martian soil [17]. A sample on the basis of sodium chloride ( $\text{NaCl}$ ) was prepared in order to measure chlorine gamma-ray lines.

Examples of the gamma-ray spectra measured in our experiment are given in Figs. 3–8. A list of gamma-ray lines for each of the gamma-ray spectrometers is presented in Table 2. These lines mostly correspond to reactions induced by radiative neutron capture, but there are several lines associated with products of inelastic fast-neutron scattering off  $^{47}\text{Ti}$  (984 keV), Ca (3737 keV), and  $^{28}\text{Si}$  (1779 keV) nuclei. By convention, the whole set of measured gamma-ray lines from samples prepared as analogs of celestial-body soil can be partitioned into two groups. The first group comprises lines that are present in the spectra of both gamma-ray spectrometers (HPGe and  $\text{CeBr}_3$ ). Lines of the second group were found



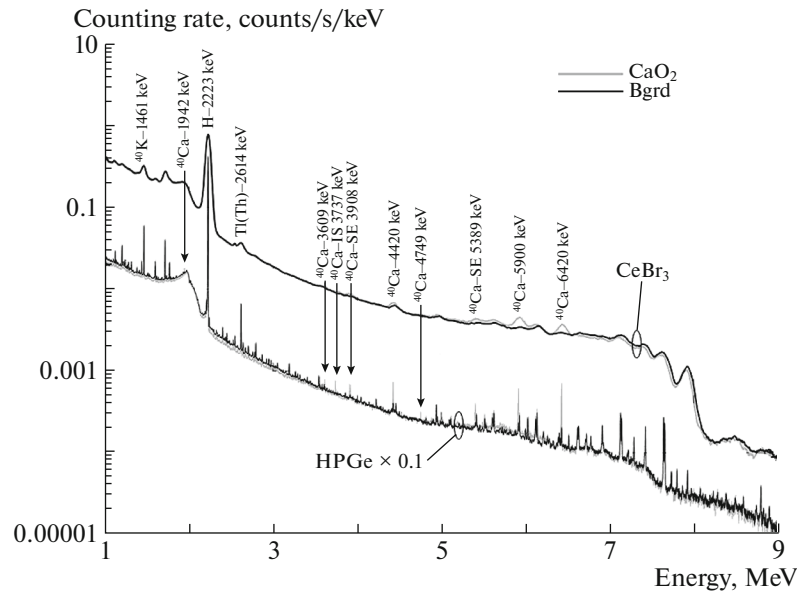


Fig. 8. As in Fig. 7, but for a  $\text{CaO}_2$  sample.

only in the spectrum measured by the germanium gamma-ray spectrometer.

A NaCl sample is of particular interest. Chlorine is known to have a large cross section for thermal-neutron capture. As a consequence, it exhibits a set of intense gamma-ray lines associated with excited neutron-capture products and distributed over a broad energy range (see Fig. 4). All gamma-ray lines (with the exception of the line at 1165 keV) of this isotope were detected by the two gamma-ray spectrometers used. The set of gamma-ray lines detected for the NaCl sample is in perfect agreement with the gamma-ray lines found during the calibration of the gamma-ray station at Czech Technical University (Prague) [14].

A target on the basis of titanium oxide ( $\text{TiO}_2$ ) is also of interest from the point of view of future space-science studies devoted to the gamma-ray spectroscopy of celestial bodies, since titanium may enter into the composition of both planet-surface soil and spacecraft material. Among nonferrous metals, titanium nuclei possess one of the largest cross sections for neutron capture and, as a consequence, emit intense gamma-ray lines. Obviously, the gamma-ray lines of titanium nuclei in the spacecraft structure are identical to gamma-ray lines of this element in celestial-body matter. This coincidence hinders a direct determination of the titanium concentration in the soil of the celestial body under study, since, for this, one needs the photon flux in the gamma-ray lines directly from the surface of this body. Therefore, the so-called background spectrum associated with intrinsic spacecraft radiation should be subtracted from the spectrum measured onboard spacecraft. It is

necessary to measure this spectrum for a spacecraft irradiated with GCR particles when the spacecraft is far from the celestial body under study and to correct it thereupon with allowance for the weakening of the total GCR flux in the immediate vicinity of this body or directly at its surface. As a result, one would obtain the gamma-ray spectrum corresponding to radiation from the celestial-body surface, and the intensity of the gamma-ray lines from titanium would reflect the concentration of its nuclei in soil. An example of the gamma-ray background model developed for the gamma-ray spectrometer installed onboard the Lunar Prospector spacecraft is presented in [7].

Figure 5 shows the spectra obtained for our titanium-oxide sample, which contain basic capture gamma-ray lines of titanium. Mostly, they were detected by both gamma-ray spectrometers. The set of the strongest lines emitted in the reactions induced by neutron capture by titanium nuclei lies in the energy range between 5 and 7 MeV.

The silicon isotope  $^{28}\text{Si}$  is among the main rock-forming elements of the surfaces of planets belonging to Earth's group. Measurements performed with a silicon-oxide sample prepared as an analog of celestial-body soil showed that three of the four lines recorded by the HPGe-based gamma-ray spectrometer were also detected by the gamma-ray spectrometer on the basis of the  $\text{CeBr}_3$  crystal. These are the 3540-, 4423- (SE), and 4934-keV gamma lines (Fig. 7). The line at the energy of 4934 keV is the strongest. It can be used as the main reference gamma-ray line in estimating the amount of silicon in the substance of celestial-body surfaces.

**Table 2.** List of samples and characteristic gamma-ray lines detected by the gamma-ray spectrometer on the basis of CeBr<sub>3</sub> and HPGe

| No.                      | Sample           | Mass, g | Basic gamma-ray lines<br>(isotope, energy, keV) | CeBr <sub>3</sub>              | HPGe |
|--------------------------|------------------|---------|---|--------------------------------|------|
| 1                        | NaCl             | 1345    | <sup>35</sup> Cl—1165                           | —                              | +    |
|                          |                  |         | <sup>35</sup> Cl—1955                           | +                              | +    |
|                          |                  |         | <sup>35</sup> Cl—2864                           | + weak                         | +    |
|                          |                  |         | <sup>35</sup> Cl—3062                           | + weak                         | +    |
|                          |                  |         | <sup>35</sup> Cl—5600 SE                        | +                              | +    |
|                          |                  |         | <sup>35</sup> Cl—6111 SE                        | 1.000                          | +    |
|                          |                  |         | <sup>35</sup> Cl—6620                           | +                              | +    |
|                          |                  |         | <sup>35</sup> Cl—6903 SE                        | +                              | +    |
|                          |                  |         | <sup>35</sup> Cl—7414                           | +                              | +    |
|                          |                  |         | <sup>35</sup> Cl—7790                           | 0.190                          | +    |
|                          |                  |         | <sup>35</sup> Cl—8068 SE                        | + weak                         | +    |
|                          |                  |         | <sup>35</sup> Cl—8579                           | 0.088                          | +    |
|                          |                  |         | 2   | Al <sub>3</sub> O <sub>3</sub> | 1185 |
| <sup>27</sup> Al—4133    | —                | + weak  |   |                                |      |
| <sup>27</sup> Al—4734    | —                | + weak  |   |                                |      |
| <sup>27</sup> Al—7213 SE | + weak           | +       |   |                                |      |
| <sup>27</sup> Al—7724    | + weak           | +       |   |                                |      |
| 3                        | TiO <sub>2</sub> | 850     | <sup>47</sup> Ti—984 IS                         | + weak                         | +    |
|                          |                  |         | <sup>48</sup> Ti—1382                           | 1.000                          | +    |
|                          |                  |         | <sup>48</sup> Ti—1586                           | —                              | +    |
|                          |                  |         | <sup>48</sup> Ti—3027                           | —                              | +    |
|                          |                  |         | <sup>48</sup> Ti—3476                           | —                              | +    |
|                          |                  |         | <sup>48</sup> Ti—3734                           | —                              | +    |
|                          |                  |         | <sup>48</sup> Ti—3923                           | —                              | +    |
|                          |                  |         | <sup>48</sup> Ti—4370 SE                        | —                              | +    |
|                          |                  |         | <sup>48</sup> Ti—4881                           | —                              | +    |
|                          |                  |         | <sup>48</sup> Ti—4967                           | —                              | +    |
|                          |                  |         | <sup>48</sup> Ti—5396 DE                        | + с.л.                         | +    |
|                          |                  |         | <sup>48</sup> Ti—5738 DE                        | —                              | +    |
|                          |                  |         | <sup>48</sup> Ti—5907 SE                        | 0.272                          | +    |
|                          |                  |         | <sup>48</sup> Ti—6249 SE                        | 0.240                          | +    |
|                          |                  |         | <sup>48</sup> Ti—6418                           | 0.265                          | +    |
|                          |                  |         | <sup>48</sup> Ti—6556                           | —                              | +    |
|                          |                  |         | <sup>48</sup> Ti—6760                           | 0.572                          | +    |
| 4                        | MnO <sub>2</sub> | 1100    | <sup>55</sup> Mn—847                            | +                              | +    |
|                          |                  |         | <sup>55</sup> Mn—1810                           | + weak                         | +    |
|                          |                  |         | <sup>55</sup> Mn—21135                          | —                              | +    |
|                          |                  |         | <sup>55</sup> Mn—3409                           | —                              | +    |
|                          |                  |         | <sup>55</sup> Mn—5014                           | +                              | +    |
|                          |                  |         | <sup>55</sup> Mn—5181                           | +                              | +    |
|                          |                  |         | <sup>55</sup> Mn—5527                           | +                              | +    |
|                          |                  |         | <sup>55</sup> Mn—5920                           | —                              | +    |
|                          |                  |         | <sup>55</sup> Mn—6784                           | —                              | +    |
|                          |                  |         | <sup>55</sup> Mn—7058                           | +                              | +    |
|                          |                  |         | <sup>55</sup> Mn—7159                           | —                              | +    |
|                          |                  |         | <sup>55</sup> Mn—7244                           | +                              | +    |
|                          |                  |         | <sup>55</sup> Mn—7270                           | —                              | +    |

On the basis of data from the CeBr<sub>3</sub>-based scintillation gamma-ray spectrometer for five samples from NaCl, SiO<sub>2</sub>, CaO<sub>2</sub>, Cr<sub>2</sub>O<sub>3</sub>, and TiO<sub>2</sub>, we selected

the strongest gamma-ray lines of the respective elements, requiring that the closest lines of other elements not overlap them (see Table 2). This set can

Table 2. End

| No. | Sample                         | Mass, g | Basic gamma-ray lines<br>(isotope, energy, keV) | CeBr <sub>3</sub> | HPGe   |
|-----|--------------------------------|---------|---|-------------------|--------|
| 5   | Cr <sub>2</sub> O <sub>3</sub> | 1440    | <sup>50</sup> Cr—749                            | —                 | +      |
|     |                                |         | <sup>53</sup> Cr—835                            | —                 | +      |
|     |                                |         | <sup>53</sup> Cr—1785                           | —                 | +      |
|     |                                |         | <sup>53</sup> Cr—2239                           | —                 | +      |
|     |                                |         | <sup>53</sup> Cr—3720                           | —                 | +      |
|     |                                |         | <sup>53</sup> Cr—5107 SE                        | —                 | +      |
|     |                                |         | <sup>53</sup> Cr—5618                           | +                 | +      |
|     |                                |         | <sup>53</sup> Cr—6589                           | +                 | +      |
|     |                                |         | <sup>53</sup> Cr—6646                           | +                 | +      |
|     |                                |         | <sup>53</sup> Cr—7100                           | —                 | +      |
|     |                                |         | <sup>53</sup> Cr—7427 SE                        | +                 | +      |
|     |                                |         | <sup>53</sup> Cr—7938                           | +                 | +      |
|     |                                |         | <sup>53</sup> Cr—8483                           | +                 | +      |
|     |                                |         | <sup>53</sup> Cr—8511                           | +                 | +      |
|     |                                |         | <sup>53</sup> Cr—8884                           | 1.000             | +      |
| 6   | CaO <sub>2</sub>               | 1000    | <sup>53</sup> Cr—9208 SE                        | 0.317             | +      |
|     |                                |         | <sup>53</sup> Cr—9719                           | 0.339             | +      |
|     |                                |         | <sup>40</sup> Ca—1943                           | —                 | +      |
|     |                                |         | <sup>40</sup> Ca—3610                           | —                 | +      |
|     |                                |         | <sup>40</sup> Ca—3737 IS                        | —                 | +      |
|     |                                |         | <sup>40</sup> Ca—3908 SE                        | + weak            | +      |
|     |                                |         | <sup>40</sup> Ca—4419                           | 0.500             | +      |
|     |                                |         | <sup>40</sup> Ca—4749                           | —                 | +      |
|     |                                |         | <sup>40</sup> Ca—5900                           | 0.809             | +      |
|     |                                |         | <sup>40</sup> Ca—6420                           | 1.000             | +      |
| 7   | SiO <sub>2</sub>               | 1390    | <sup>28</sup> Si—1779 IS                        | —                 | +      |
|     |                                |         | <sup>28</sup> Si—3540                           | 1.000             | +      |
|     |                                |         | <sup>28</sup> Si—4423 SE                        | 0.340             | +      |
|     |                                |         | <sup>28</sup> Si—4934                           | 0.628             | +      |
|     |                                |         | <sup>28</sup> Si—6380                           | —                 | —      |
|     |                                |         | <sup>28</sup> Si—8467                           | —                 | —      |
| 8   | P <sub>2</sub> O <sub>5</sub>  | 940     | <sup>31</sup> P—3523                            | —                 | + weak |
|     |                                |         | <sup>31</sup> P—3900                            | —                 | +      |
|     |                                |         | <sup>31</sup> P—4671                            | —                 | +      |
|     |                                |         | <sup>31</sup> P—6786                            | —                 | +      |
| 10  | Soil 1                         | 1605    | <sup>28</sup> Si—1779                           | + weak            | +      |
|     |                                |         | <sup>28</sup> Si—3540                           | +                 | +      |
|     |                                |         | <sup>28</sup> Si—4423 SE                        | +                 | +      |
|     |                                |         | <sup>28</sup> Si—4934                           | +                 | +      |
|     |                                |         | <sup>27</sup> Al—7724                           | —                 | +      |
| 11  | Soil 2                         | 1585    | <sup>28</sup> Si—1779                           | + weak            | +      |
|     |                                |         | <sup>28</sup> Si—3540                           | +                 | +      |
|     |                                |         | <sup>28</sup> Si—4423 SE                        | —                 | +      |
|     |                                |         | <sup>28</sup> Si—4934                           | +                 | +      |
|     |                                |         | <sup>27</sup> Al—7724                           | —                 | +      |

Weak stands for a weak line.

be called a set of reference gamma-ray lines for determining the content of respective elements in celestial-body matter.

For the selected reference gamma-ray lines, their physical intensities (in photon cm<sup>-2</sup> s<sup>-1</sup> units) at the position of the cerium-bromide detector were esti-

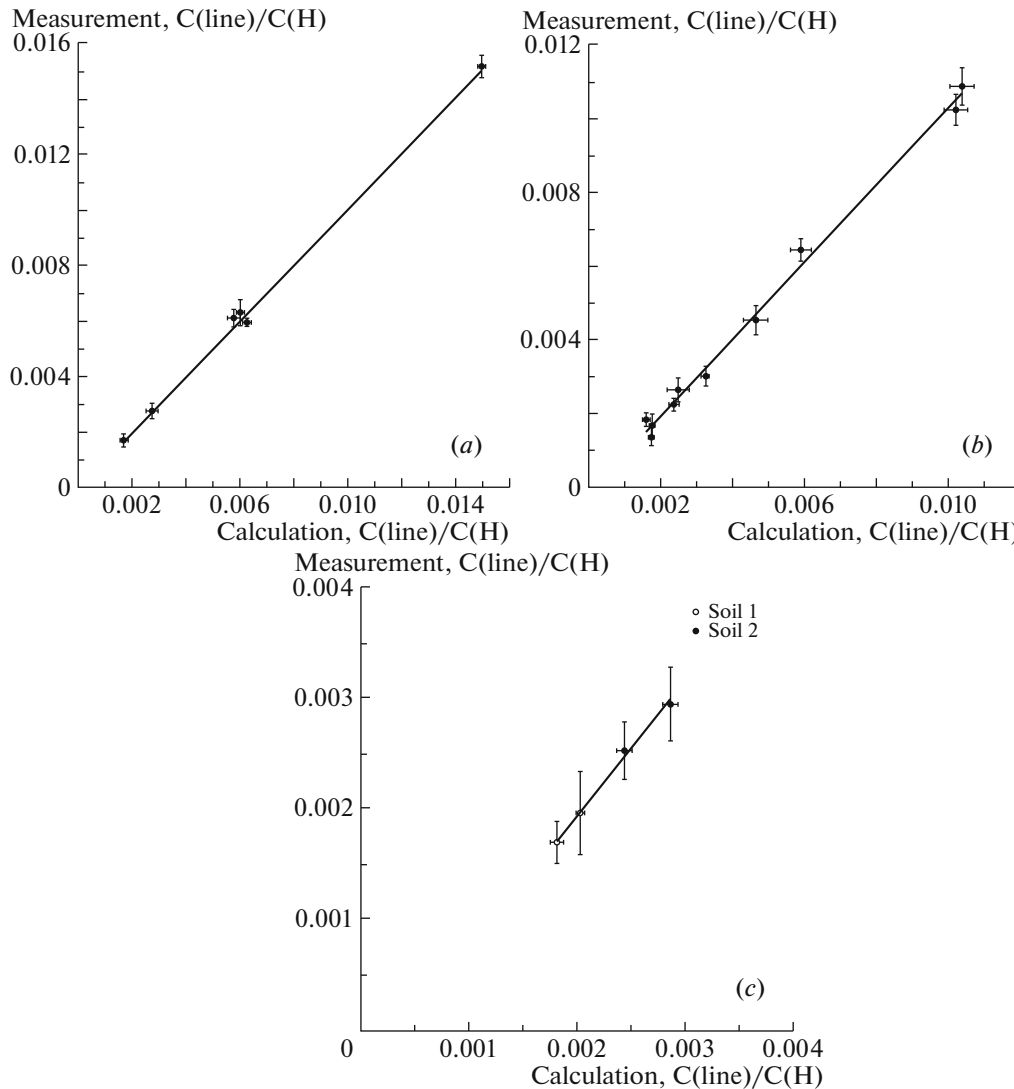


**Fig. 9.** Intensities of the measured gamma-ray lines versus the intensities of the calculated gamma-ray lines of the scintillation gamma-ray spectrometer on the basis of  $\text{CeBr}_3$  that were normalized to the 2223-keV hydrogen gamma line for (a)  $\text{TiO}_2$ , (b)  $\text{Cr}_2\text{O}_3$ , and (c) Soil 1 and Soil 2 targets.

mated on the basis of the recorded numbers of counts with allowance for the absorption of photons in the materials of the gamma-ray station and their detection efficiency. For this purpose, we used the energy dependences calculated by means of the Geant4 code [19] for absorption in water and for the efficiency of absorption in cerium bromide. The fluxes of reference gamma-ray lines for the five selected samples at the gamma-chamber center were normalized to the intensity of the strongest gamma-ray line for a given element (see Table 2).

The relative intensities of gamma-ray lines in the reference set for each element can be used to determine its content in celestial-body substances in the course of space-science experiments (for example, in an analysis of data from the MGNS and LGNS experiments, where gamma-ray spectrometers on the

basis of a  $\text{CeBr}_3$  crystal will be employed to study the composition of the surfaces of Mercury and the Moon, respectively). The measured intensities of reference lines of individual elements will be compared with respective numerical estimates obtained with allowance for absorption in celestial-body matter and upon taking into account the detection efficiency. The mass fraction of an element should be a free parameter that is evaluated by requiring agreement between the measured and calculated intensities.

In order to obtain reliable estimates of the composition of celestial-body matter, it is necessary to test codes for a numerical simulation of the intensities of gamma-ray lines; in particular, one should verify neutron-capture and photon-scattering cross sections used as input data in respective calculations. This verification of code packages should precede the

implementation of respective space-science experiments. For samples in which tested elements have known mass fractions, numerical calculations of the intensities of basic reference gamma-ray lines should be performed, whereupon the results of these calculations should be confirmed by physical measurements.

In order to perform a numerical simulation of the results of measurements at EF-NP-03, we employed the dedicated ACPS-LI-03 (Analysis of Composition of Planet Substances—Laboratory Investigations) code package intended for simulating spectral properties of secondary gamma ray from samples prepared as analogs of celestial-body matter and irradiated with steady-state thermal-neutron fluxes. This package is based on the MCNPX 2.7e code for performing nuclear-physics calculations with the aid of the ENDF/B-VII.0 and ENDF/B-VI libraries of, respectively, neutron-induced and photoatomic processes [20, 21]. The numerical model used included a description of a parallelepiped  $50 \times 56 \times 56$  cm in size filled with 110 l of  $H_2O$ ; a sample simulating celestial-body matter; a  $^{252}Cf$  neutron source within the sample; the concrete walls, floor, and ceiling of the laboratory hall; and models of the detectors based on  $CeBr_3$  and HPGe crystals. In order to simplify our description of the geometry of the problem being considered, auxiliary laboratory equipment present in the hall was not included in this numerical model. The gamma-ray lines associated with the decay of natural radioactive elements were also disregarded since this was beyond the scope of the simulation. The spectra of the numbers of counts were simulated numerically upon taking into account the energy resolution of the detectors used, which was determined earlier in the course of dedicated calibration measurements.

Thus, a numerical simulation of gamma-ray fluxes and spectra of counts recorded by the detectors on the basis of  $CeBr_3$  and HPGe crystals at a distance of 1 m from the center of the gamma-ray station was performed for each experimental measurement of samples at EF-NP-03. Examples of the simulated spectra for the  $NaCl$ ,  $TiO_2$ , and  $Cr_2O_3$  samples prepared as analogs of celestial-body substances are given in Figs. 4, 5, and 6, respectively.

In order to compare the results of measurements and numerical simulations of spectral properties of secondary gamma rays from the tested samples, we plotted graphs of the respective intensities of the calculated and measured gamma-ray lines. Examples of such a comparison for the  $TiO_2$  and  $Cr_2O_3$  samples are given in Fig. 9. In plotting these dependences, the intensities of the gamma-ray lines in each spectrum were normalized to the intensity of the 2223 keV hydrogen gamma-ray line associated with neutron absorption in water filling the tank of the gamma-ray station. Similar graphs intended for a comparison of

the above type were plotted for the Soil 1 and Soil 2 samples (see Fig. 9). These graphs show that there is nearly perfect agreement (within statistical uncertainties) between the results of our numerical simulation and data from experimental measurements. This means that the code packages developed for numerically simulating fluxes of neutron-capture gamma rays from rock-forming elements of celestial-body matter may be applied to processing and analysis of data from space-science experiments devoted to the gamma-ray spectroscopy of planets and small bodies of the Solar System.

#### 4. CONCLUSIONS

The EF-NP-03 laboratory setup featuring two independent gamma-ray spectrometers has been created in order to perform measurements with samples prepared as analogs of celestial-body matter. These samples include chemical elements that are the main rock-forming elements in the surface layers of the the Moon and planets of Earth's group (Mars, Mercury, and Venus). The results of respective laboratory measurements were used to create a database of reference gamma-ray lines of basic rock-forming elements that can be identified by means of a gamma-ray spectrometer on the basis of a  $CeBr_3$  scintillation crystal. For the database of these lines, the interested reader is referred to the web site <https://np.cosmos.ru/rmf/>.

In addition, a numerical model of the aforementioned experimental setup was created on the basis of the ACPS-Li-03 code package developed for this purpose. This numerical model permitted calculating spectral properties of secondary gamma rays from samples mimicking celestial-body matter. We have shown that the results of numerical calculations agree well with experimental data. Dedicated ACPS-Planet code packages for simulating conditions of space-science experiments will be developed on the basis of the ACPS-Li-03 package.

The results of the present study will be used in the future to analyze and interpret data obtained in the MGNS space-science experiments aimed at an orbital survey of the surface of Mercury within the ESA BepiColombo project [12] and in the LGNS experiment aimed at an orbital survey of the Moon's surface within the Russian Luna-26 project.

#### ACKNOWLEDGMENTS

This work was supported by the Russian Science Foundation (grant no. 14-22-00249). The work of the authors from Institute of Experimental and Applied Physics, Czech Technical University in Prague (Czech Republic), was supported by the European Regional Development Fund (grant no. CZ.02.1.01 / 0.0 / 0.0 / 16\_013 / 0001785).

## REFERENCES

1. A. P. Vinogradov, Yu. A. Surkov, G. M. Chernov, *Kosm. Issled.* **4**, 871 (1966).
2. A. P. Vinogradov, Yu. A. Surkov, and L. P. Moskaleva in *Moon and Planets II*, Ed by A. Dollfus (North-Holland, Amsterdam, 1968), p. 77.
3. W. V. Boynton, W. C. Feldman, I. G. Mitrofanov, L. G. Evans, R. C. Reedy, S. W. Squyres, R. Starr, J. I. Trombka, C. d'Uston, J. R. Arnold, P. A. J. Englert, A. E. Metzger, H. Wänke, J. Brückner, D. M. Drake, C. Shinohara, et al., *Space Sci. Rev.* **110**, 37 (2004).
4. J. Masarik and R. C. Reedy, *J. Geophys. Res.* **101**, 18891 (1996).
5. Yu. A. Surkov, F. F. Kirnozov, V. N. Glazov, A. G. Dunchenko, L. P. Tatsy, and O. P. Sobornov, in *Proceedings of the 17th Lunar and Planetary Science Conference, Houston, USA, Mar. 17–21, 1986*; *J. Geophys. Res.* **92**, E537 (1987).
6. L. G. Evans, R. C. Reedy, R. D. Starr, K. E. Kerry, and W. V. Boynton, *J. Geophys. Res.* **111**, E03S04 (2006).
7. T. H. Prettyman, J. J. Hagerty, R. C. Elphic, W. C. Feldman, D. J. Lawrence, G. W. McKinney, and D. T. Vaniman, *J. Geophys. Res.* **111**, E12007 (2006).
8. L. G. Evans, P. N. Peplowski, E. A. Rhodes, D. J. Lawrence, T. J. McCoy, L. R. Nittler, S. C. Solomon, A. L. Sprague, K. R. Stockstill-Cahill, R. D. Starr, S. Z. Weider, W. V. Boynton, D. K. Hamara, and J. O. Goldsten, *J. Geophys. Res.* **117**, E00L07 (2012).
9. J. O. Goldsten, E. A. Rhodes, W. V. Boynton, W. C. Feldman, D. J. Lawrence, J. I. Trombka, D. M. Smith, L. G. Evans, J. White, N. W. Madden, P. C. Berg, G. A. Murphy, R. S. Gurnee, K. Strohbahn, B. D. Williams, E. D. Schaefer, et al., *Space Sci. Rev.* **131**, 339 (2007).
10. N. Hasebe, E. Shibamura, T. Miyachi, T. Takashima, M. Kobayashi, O. Okudaira, N. Yamashita, S. Kobayashi, Y. Karouji, M. Hareyama, S. Kodaira, K. Hayatsu, K. Iwabuchi, S. Nemoto, K. Sakurai, S. Komatsu, et al., *Trans. Space Technol. Jpn.* **7**, Pk\_35 (2010).
11. I. V. Khodyuk, F. G. A. Quarati, M. S. Alekhin, and P. Dorenbos, arXiv: 1209.5278.
12. I. G. Mitrofanov, A. S. Kozyrev, A. Konovalov, M. L. Litvak, A. A. Malakhov, M. I. Mokrousov, A. B. Sanin, V. I. Tret'ykov, A. V. Vostrukhin, Yu. I. Bobrovnikskij, T. M. Tomilina, L. Gurvits, and A. Owens, *Planet. Space Sci.* **58**, 116 (2010).
13. A. Kozyrev, I. Mitrofanov, A. Owens, F. Quarati, J. Benkhoff, B. Bakhtin, F. Fedosov, D. Golovin, M. Litvak, A. Malakhov, M. Mokrousov, I. Nuzhdin, A. Sanin, V. Tret'yakov, A. Vostrukhin, G. Timoshenko, et al., *Rev. Sci. Instrum.* **87**, 085112 (2016).
14. C. Granja, T. Slavicek, M. Kroupa, A. Owens, S. Pospisil, Z. Janout, M. Kralik, J. Solc, and O. Valach, *Nucl. Instrum. Methods Phys. Res., Sect. A* **771**, 1 (2015).
15. Yu. A. Alexandrov, W. I. Furman, A. V. Ignatyuk, M. V. Kazarnovsky, V. Yu. Konovalov, N. V. Kornilov, L. B. Pikelner, V. I. Plyaskin, Yu. P. Popov, H. Rauch, W. Waschkowski, and Yu. S. Zamyatnin, *Low Energy Neutron Physics*, Ed. by H. Schopper (Springer, Berlin, 2000), Part 1.
16. M. L. Litvak, D. V. Golovin, A. B. Kolesnikov, A. A. Vostrukhin, M. V. D'yachkova, A. S. Kozyrev, I. G. Mitrofanov, M. I. Mokrousov, and A. B. Sanin, *Solar Syst. Res.* **51**, 171 (2017).
17. R. Rieder, T. Economou, H. Wanke, A. Turkevich, J. Crisp, J. Breckner, G. Dreibus, and H. Y. McSween, Jr., *Science (Washington, DC, U. S.)* **278**, 1771 (1997).
18. G. J. Taylor and E. R. D. Scott, in *Treatise on Geochemistry*, Ed. by H. D. Holland and K. K. Turekian (Elsevier, Amsterdam, 2004), p. 477.
19. S. Agostinelli, J. Allison, K. Amako, J. Apostolakis, H. Araujo, P. Arce, M. Asai, D. Axen, S. Banerjee, G. Barrand, F. Behner, L. Bellagamba, J. Boudreau, L. Broglia, A. Brunengo, H. Burkhardt, et al., *Nucl. Instrum. Methods Phys. Res.* **506**, 250 (2003).
20. *MCNPX User's Manual, Version 2.7.0*, Ed. by D. B. Pelowitz, Los Alamos Natl. Laboratory Report No. LA-CP-11-00438 (Los Alamos Natl. Laboratory, Los Alamos, 2011).
21. M. B. Chadwick, M. Herman, P. Obložinský, M. E. Dunn, Y. Danon, A. C. Kahler, D. L. Smith, B. Pritychenko, G. Arbanas, R. Arcilla, R. Brewer, D. A. Brown, R. Capote, A. D. Carlson, Y. S. Cho, H. Derrien, et al., *Nucl. Data Sheets* **112**, 2887 (2011).